JBC Papers in Press. Published on March 4, 2016 as Manuscript M115.699850
The latest version is at http://www.jbc.org/cgi/doi/10.1074/jbc.M115.699850

Oxidant-induced interprotein disulfide formation in cardiac DJ-1 occurs via an interaction with peroxiredoxin 2*

Mariana Fernandez-Caggiano[1], Ewald Schröder[1], Hyun-Ju Cho[1], Joseph Burgoyne[1]

Javier Barallobre-Barreiro[2], Manuel Mayr[2] and Philip Eaton[1]

[1] King's College London, Cardiovascular Division, The British Heart Foundation Centre of Excellence, The Rayne Institute, St Thomas' Hospital, London SE1 7EH, United Kingdom

[2] King's College London, Cardiovascular Division, The British Heart Foundation Centre of Excellence, The James Black Centre, King's College Hospital, London SE5 9NU, United Kingdom

*Running title: Thiol modifications in cardiac DJ-1

To whom correspondence should be addressed: Philip Eaton, Cardiovascular Division, King's College London. The Rayne Institute, St. Thomas' Hospital, London SE1 7EH, United Kingdom. Tel: (+44)20 7188 0969 Fax: (+44)20 7188 0970 E-mail philip.eaton@kcl.ac.uk

Keywords: DJ-1 (PARK7), peroxiredoxin 2, redox regulation, oxidative stress, heart

ABSTRACT

The role and responses of the dimeric DJ-1 protein to cardiac oxidative stress is incompletely understood. H_2O_2 induced a 50 kDa DJ-1 interprotein homodimer disulfide, known to form between Cys53 on each subunit. A trimeric 75 kDa DJ-1 complex, which mass spectrometry showed contained 2-Cys peroxiredoxin, also formed and preceded appearance of the disulfide dimer. These observations may represent peroxiredoxin sensing and transducing the oxidant signal to DJ-1. The dimeric disulfide DJ-1 complex was stabilised by auranofin, suggesting that thioredoxin recycles it in cells. Higher concentrations of H_2O_2 concomitantly induced DJ-1 Cys106 hyperoxidation (sulfination or sulfonation) in myocytes, perfused heart or HEK cells. An oxidation-resistant C53A DJ-1 showed potentiated H_2O_2-induced Cys106 hyperoxidation. DJ-1 also formed multiple disulfides with unknown target proteins during H_2O_2 treatment, whose formation were also potentiated in cells expressing the C53A mutant. This suggests that the inter subunit disulfide induces a conformational change that limits Cys106 forming hetero- disulfide protein complexes or from hyperoxidising. High concentrations of H_2O_2 also induced cell death, with DJ-1 Cys106 sulfonation appearing causal in these events, as expression of C53A DJ-1 both enhanced Cys106 sulfonation and cell death. Nonetheless, expression of a C106A DJ-1 mutant that fully prevents hyperoxidation also exacerbated cell death responses to H_2O_2. A rational explanation for these findings is that DJ-1 Cys106 forms disulfides with target proteins to limit oxidant-induced cell death. However, when Cys106 is hyperoxidised formation of these potentially protective heterodimeric disulfide complexes are limited and so cell death is exacerbated.

Oxidative stress is associated with a net increase in concentration of reactive oxygen species (ROS) and is implicated in the pathogenesis of heart disease, including ischemia/reperfusion injury, cardiac hypertrophy, and heart failure. ROS may be injurious by causing oxidative damage or dysregulating homeostatic redox signalling pathways. Antioxidant ROS-neutralizing defence mechanisms maintain the cellular environment in a reduced condition, limiting oxidation of proteins and other biomolecules. Parkinson protein 7 (DJ-1) is one of the most abundant redox-sensitive proteins within the heart. However, little is known about its response during cardiac oxidative stress.

Human DJ-1 contains 189 amino acid residues and exists as a homodimer of two ~20 kDa subunits (1). DJ-1 was first identified as an oncogene (2), and has since been described as a

causative gene for early-onset Parkinson disease (3,4). Although DJ-1 has protease (5-7) or chaperone (8,9) activities, most studies have focused on its protective role against oxidative stress (10-15). Knockout of the DJ-1 gene enhances hydrogen peroxide (H_2O_2) and (1-methyl-4-phenyl-1,2,3,6-tetrahydropyridine) - mediated cell death. Furthermore, examination of mitochondria from KO mice revealed that DJ-1 acts as an atypical peroxiredoxin-like peroxidase which has the ability to scavenge H_2O_2 (16). DJ-1 can also bind to mRNA encoding factors such as protein 53 (p53) (20) and proteins involved in glutathione synthesis (17), but when oxidised it releases these factors to facilitate translation of oxidative stress response proteins. For all these reasons DJ-1 is generally considered to be an antioxidant protein.

The cysteine residues in this protein are crucial for its cytoprotective activity (18,19). Human DJ-1 contains three cysteine residues, Cys46, Cys53 and Cys106. Cys106 is the most conserved cysteine and is a critical mediator of many of DJ-1 functions (20). The Cys106 thiol residue has an acid dissociation constant (pKa) of 5.4 (21), meaning it is predominantly ionised at physiological pH - explaining it reactivity with oxidants (16,22). Cysteine residues can be oxidized to three distinct species by the cumulative additions of oxygen; successively forming cysteine-sulfenic (-SOH), -sulfinic (-SO_2H) and -sulfonic (-SO_3H) acid. These three species have different physico-chemical characteristics. Peroxide-induced formation of a disulfide bond between two cysteine thiols is generally mediated by sulfenic acid formation or by thiol-disulfide exchange (23). Such post-translational oxidative modifications may lead to perturbations in conformation, stability, molecular interactions or activity of proteins such as DJ-1, providing a potential mechanism of their redox regulation.

Mammalian peroxiredoxins (Prdx) proteins are peroxidases, comprised of three main groups according to the number of active cysteines and their positional variation, including the typical 2-Cys Prdxs, the atypical 2-Cys Prdxs and the 1-Cys Prdxs (24,25). Dimeric Prdx1, Prdx2, Prdx3 and Prdx4 are typical 2-Cys Prdxs in which the peroxidatic thiol reacts with H_2O_2 to form a sulfenic acid, which is then 'attacked' by a resolving cysteine on the other monomer in the functional pair. The resulting Prdx disulfide dimer is reduced by the disulfide reductase thioredoxin (Trx) to regenerate reduced Prdx proteins capable of decomposing another molecule of H_2O_2 (26). When the Trx reduces the oxidised Prdx, it does so at the expense of becoming oxidised itself via a thiol disulfide-exchange reaction. Prdx may also thiol-disulfide exchange with other proteins and induce disulfide bond formation, thereby potentially modifying their activities. For example, Prxd4 directly oxidises protein disulfide isomerase within the endoplasmic reticulum thereby increasing the oxidative folding of substrates such as RNase A (27). Similarly, Prdx2 (~22 kDa) attenuates the transcriptional activity of STAT3 likewise through disulfide-bond formation (28). In this way Prdx serves as a sensor that 'picks up' increases in a cellular oxidant signal by virtue of disulfide bond formation. This signal can then transduced by the aforementioned thiol-disulfide exchange reaction to induce oxidation of a target protein whose activity may be redox-state dependent. In this way proteins which may not directly react with oxidants may still become oxidised, but indirectly with Prdx oxidation serving as an intermediate step.

The redox state of DJ-1 in HEK cells, isolated cardiomyocytes or isolated hearts exposed to increasing concentrations of H_2O_2 was shown to undergo complex redox state changes. Transfection studies with C53A or C106A DJ-1 mutants show the oxidation state of either of these individual cysteines impacts on the susceptibility of the other to oxidation, with interventions that promote hyperoxidation of Cys106 exacerbating H_2O_2-induced cell death. H_2O_2-induced DJ-1 disulfide formation was found to occur via a mechanism in which Prdx2 first reacts with the oxidant to form a disulfide, which is then transmitted to DJ-1, likely via a thiol-disulfide exchange reaction.

EXPERIMENTAL PROCEDURES

This investigation was performed in accordance with the Home Office Guidance on the Operation of the Animals (Scientific Procedures) Act 1986, published by Her Majesty's Stationery Office (London, UK). Animals were maintained humanely in compliance with the "Principles of Laboratory Animal Care" formulated by the National Society for Medical Research and the Guide for Care and Use of Laboratory Animals prepared by the National Academy of Sciences and published by

the National Institutes of Health (NIH Pub. No. 85-23, revised 1985). All animal protocols were approved both by the local King's College Ethical Review Process Committee and by the UK Government Home Office (Animals Scientific Procedures Group).

Studying DJ-1 oxidation in isolated rat cardiomyocytes or hearts perfused with H_2O_2

Ventricular myocytes were isolated from hearts of male Wistar rats (body weight, 200–250 g) as described previously (29). In brief, the rats were anesthetized with pentobarbitone sodium (40 mg intraperitoneally) and injected with sodium heparin (200 IU) via the femoral vein. Hearts were excised and perfused for 5 min with modified HEPES-Krebs solution (pH 7.3 at 37 °C) containing 0.75 mmol/L $CaCl_2$. Then, hearts were consecutively perfused with Ca^{2+}-free HEPES-Krebs solution containing 100 µmol/L EGTA (4-10 min) and with HEPES-Krebs solution containing 100 mmol/L $CaCl_2$ and 1 mg/ml type II collagenase (Worthington) (8 min). Subsequently the ventricles were removed and cut into small pieces. Single cells were separated from undigested ventricular tissue by filtering through nylon gauze and stored in the taurine-containing solution until the myocytes settle down. The isolated myocytes were cultured in pre-laminated 6-well culture plates or on individual 3.5 cm dishes for confocal microscopy with modified M199 culture medium (Invitrogen) containing 2 mmol/L creatine, 2 mmol/L carnitine and 5 mmol/L taurine plus 100 IU/ml penicillin/streptomycin. The culture medium was replaced after 2 hours and the cells were maintained overnight. The next day cardiomyocytes were treated with H_2O_2 (0-200 µM) for 10 min or with auranofin (1-3 µg, Sigma).

Rat hearts were also isolated, cannulated and perfused in Langendorff mode at a constant flow of 12 ml/min as follows: 30 min of aerobic perfusion with bicarbonate buffer followed by 5 min of perfusion with 0–500 µM H_2O_2 in bicarbonate buffer. At the end of the perfusion protocol, hearts were frozen and stored in liquid nitrogen until further analysis. Hearts were homogenised using a Polytron-style tissue grinder in cold buffer containing 100 mM Tris-HCl pH 7.2, 100 mM maleimide and protease inhibitors (Complete C, Roche).

In vitro preparation of WT and DJ-1 cysteine mutants and Prdx 2

HEK 293T cells were maintained in DMEM supplemented with 10% FBS and transfected using Lipofectamine 2000 (Invitrogen) according to the manufacturer instructions. The mammalian expression plasmids for DJ-1 WT and mutants were acquired from Addgene (DJ-1 WT plasmid #29416, DJ-1 C53A plasmid #29419 and DJ-1 C106A plasmid #29409). The Prdx2 plasmid (#31338, Addgene) was subcloned into a mammalian expression vector using a pcDNA™3.3-TOPO® TA Cloning® Kit (Invitrogen). Two days after transfection cells were treated with H_2O_2 (0-500 µM) for 10 min.

Immunoblotting analysis and immunoprecipitation of DJ-1

Protein samples prepared from hearts and cardiomyocytes were loaded (200 µg) and separated by SDS-PAGE using the Mini Protean 3 system (Bio-Rad) and transferred to PDVF membranes (GE Healthcare). Blots were incubated with the following primary antibodies diluted 1:000 in PBS-Tween 5% milk overnight: DJ-1 (ab18257, Abcam), V5-tag (ab27671, Abcam), Prdx2 (ab15572, Abcam) and a SO_3H-Cys106 DJ-1 antibody generated in-house as detailed below. One hour incubation with horseradish peroxidase-coupled anti-mouse (#7076, Cell Signalling) and anti-rabbit (#7074, Cell Signalling) IgG secondary antibody (diluted 1:1,000 in PBS-Tween 5% milk) was used to detect primary antibodies bound to the blot, together with enhanced chemiluminescence reagent (GE Healthcare).

Cardiomyocytes were lysed in RIPA buffer (10 mM Tris pH 7.4, 140 mM NaCl, 0.1% Triton X-100 0.1% SDS and 1% sodium deoxycholate) supplemented with protease inhibitor cocktail (Complete C, Roche). The lysates were then incubated with DJ-1 antibody (ab18257, Abcam) overnight on a rotating wheel. The next day A/G agarose beads (sc-2003, Santa Cruz) were added to the samples according to the manufacturer instructions. After 3 washes with RIPA buffer the precipitates were re-suspended in Laemmli sample buffer containing 5% β-mercaptoethanol at 95°C. In order to precipitate DJ-1 WT and cysteine mutants, HEK 293T cells

were lysed in RIPA buffer, incubated with V5-beads (A7345, Sigma) overnight and washed 3 times with RIPA buffer. Finally, precipitates were re-suspended in Laemmli sample buffer containing 5% β-mercaptoethanol.

Proteomic analysis

20 µg of protein obtained from DJ-1 immunoprecipitated from cardiomyocytes were loaded and separated on 4-12% polyacrylamide gradient gels (NuPAGE, BioRad). After electrophoresis, gels were silver stained and a 75 kDa band was excised and subjected to in-gel digestion with molecular grade trypsin (ThermoScientific, UK) using standard protocols. Tryptic peptides were separated on a nanoflow LC system (Dionex UltiMate 3000) and eluted with a 40 min, 4 step gradient (10–25%B in 35 min, 25–40% B in 5 min, 90% B in 10 min, and 2% B in 30 min where A was 2% ACN, 0.1% formic acid in HPLC H_2O and B is 90% ACN, 0.1% formic acid in HPLC H_2O). The column (Dionex PepMap C18, 25-cm length, 75 µm internal diameter, 3 µm particle size) was coupled to a nanospray source (Picoview) using RePlay (Advion) in order to obtain a technical duplicate of the LC-MS/MS. Spectra were collected from an ion trap mass analyzer (LTQ-Orbitrap XL, ThermoFisher Scientific). MS/MS peak lists were generated by extract_msn.exe and matched to a rat database (UniProtKB/Swiss-Prot, 35702 protein entries) using SEQUEST and X! Tandem. Peptide identifications were accepted if they could be established at greater than 95.0% probability as specified by the Peptide Prophet algorithm 3. Protein identifications were accepted if they could be established at greater than 99.0% probability with at least two independent peptides.

DJ-1 Cys106-SO_3H detection by immunoblotting

The active site peptide KGLIAAIC*AGPT was synthesised with sulfonic acid (cysteic acid) incorporated in place of the catalytic Cys106 (C*) [PARK7_RAT], coupled to KLH, and rabbits immunised. IgGs selective against DJ-1 sulfonylated at Cys106 were purified by affinity capture using a hyperoxidised peptide attached to a column. IgGs were eluted with sequential low and high pH washes, and the antibody described resided in the low pH elution pool.

Immunofluorescence and Proximity Ligation Assay (PLA) analysis

Cardiomyocytes and HEK 293 cells were fixed with 4% paraformaldehyde (Sigma) in PBS for 10 min at room temperature, washed in PBS and permeabilised with 0.2% Triton X-100 in PBS for 5 min. In order to avoid non-specific antibody binding the cells were incubated with blocking buffer (5 % non-specific goat serum diluted in 1 % bovine serum albumin, Tris-base 20 mmol/L, NaCl 155 mmol/L, EGTA 2 mmol/L, $MgCl_2$ 2 mmol/L, pH 7.5) for 1 hour at room temperature. Cells were incubated in primary antibody diluted (1:100) in blocking buffer overnight at 4 °C and washed with PBS the next day. For double immunofluorescence with V5-tag (ab27671, Abcam) and SO_3H-Cys106 DJ-1 antibodies, a combination of Cy3-conjugated anti-rabbit (111-165-144, Jackson ImmunoResearch) and Cy5-conjugated anti-mouse (115-177-003, Jackson ImmunoResearch) secondary antibodies were used at a 1:100 dilution for 1 hour at room temperature. Diamidine-2-phenylindole dihydrochloride (D8417, Sigma) was added with the secondary antibodies to stain the nucleus.

The in situ Proximity Ligation Assay (PLA) experiments were performed using the Duolink In Situ Red Starter Kit Mouse/Rabbit (DUO92101, Sigma) according to the manufacturer's instructions. Samples were mounted in Lisbeth's medium onto microscope slides and were analysed using confocal microscopy on an inverted microscope (Leica SP5 system) equipped with a blue diode and argon and helium neon lasers. For PLA analysis of HEK 293 T cells V5-tag (ab27671, Abcam) and His-tag (#12698, Cell Signalling) primary antibodies were use at 1:100 dilutions.

Analysis of cell death by MTT assay and apoptosis by flow cytometry in DJ-1 WT and cysteine mutants

A total of 7 X 10^6 HEK293 cells plated in a 6 well flat bottom plates were treated with 200 µM H_2O_2 for 18 hours. At the indicated time, the cells were incubated for 30 min with 0.5 mg/ml dye MTT (3-(4,5-dimethylthiazol-2-yl)-2,5-diphenyltetrazolium bromide) and then 500 µl of

stop solution (0.1N HCl, 10% Triton X100 in isopropanol) was added to each well to dissolve the formazan crystals. The absorbance at 570 nm was determined using a Gemini XPS plate reader (Molecular Devices). Triplicate wells were assayed for each condition.

For the flow cytometry protocol transfected cells were harvested, washed with PBS and incubated for 30 min with 1 µl of the reconstituted Live/Dead cell stain (#L34957, Life Technologies). After the incubation time, HEK293 cells were washed with PBS and incubated for 20 min with Annexin V-APC antibody (#A35111, Life Technologies) diluted in annexin binding buffer (#V-13246, Life Technologies) following the manufacturer's instructions. HEK 293 were washed with annexin binding buffer and re-suspended in 500 µl of fixation/ permeabilization buffer (#GAS003, Life Technologies) for 20 min. The fixation buffer was removed by washing the cells with Perm/Wash buffer (#GAS003, Life Technologies). Finally, the cells were incubated with V5-tag FITC (#R96325, Life Technologies) and cleaved caspase-3 (Asp175) (#12768S, Cell Signalling) for 30 min and washed with FACS (PBS, 2% BSA). The suspension was analyzed on a FACS Canto (BD). Data were analyzed with FlowJo version 7.6.5 (Treestar, Inc.). The median fluorescence intensities were calculated on an arbitrary scale.

Statistical analysis

The effect of H_2O_2 on the different DJ-1 mutants were analysed by a one or two-way ANOVA followed by Bonferroni post-hoc test using GraphPad Prizm 4 software. Normality was assessed by the Shapiro-Wilk test and homogeneity was assessed by a residual plot. Differences were considered significant at $P < 0.05$.

RESULTS

Oxidant-induced DJ-1 redox state alterations in cardiomyocytes and heart

Adult rat ventricular cardiomyocytes or isolated rat hearts were exposed to 0-200 or 0–500 µM H_2O_2 respectively. The cells or hearts were collected in buffer with maleimide, an alkylating agent which limits any further oxidation of cysteinyl thiols. Immunoblotting analysis of cardiomyocytes (**Fig. 1A**) or hearts (**Fig. 1B**) showed that DJ-1 migrates as a monomer under basal non-reducing conditions. However, H_2O_2 treatment induced formation of DJ-1 disulfide species which were absent when electrophoresis was performed under reducing conditions. This oxidant-induced disulfide formation occurred robustly both in cardiomyocytes (**Fig. S1A**) and in heart (**Fig. S1B**), showing a consistent banding pattern. The lower concentrations of H_2O_2 induced a 75 kDa disulfide complex, which was lost when higher levels were used, at which point a 50 kDa disulfide complex appeared. The 50 kDa band was likely to correspond to a DJ-1 disulfide dimer, consistent with conjugation of two ~25 kDa DJ-1 monomers, which are known to be proximal to each other. H_2O_2 at 100-500 µM was sufficient to oxidize Cys106 in cardiomyocytes (**Fig.1A**) or hearts (**Fig.1B**) to the sulfinic or sulfonic acid state, termed hyperoxidation. To assess the formation of these disulfide complexes in the myocardium, isolated hearts were also perfused with 1 mM diamide. Diamide also promoted the 50 and 75 kDa DJ-1 disulfide complexes (**Fig.1B**), but less efficiently than that achieved by H_2O_2.

To establish whether the redox state of DJ-1 can be regulated by the Trx system, cardiomyocytes were pre-treated with auranofin before inducing DJ-1 oxidation. Auranofin is an inhibitor of selenocysteine enzymes including thioredoxin reductase. Co-treatment with auranofin limited the amount of H_2O_2-induced 75 kDa complex and promoted the formation of the 50 kDa disulfide dimer (**Fig. 1C**).

Interaction of DJ-1 with Prdx 2

Proteins that potentially form disulfide interactions with DJ-1 following oxidant interventions to mediate the 75 kDa complex were identified (**Table 1**). This was achieved by immunoprecipitating DJ-1 from vehicle or H_2O_2-treated cardiomyocytes, resolving the sample by SDS-PAGE, excising a 75 kDa gel band piece from each sample lane and analysing each of them for constituent proteins using mass spectrometry. Consistent with mass spectrometry being very sensitive several proteins were identified in the two samples despite the immunoprecipitation step. As expected these included proteins with a mass of approximately 75 kDa, but smaller proteins such as

glyceraldehyde-3-phosphate dehydrogenase, myoglobin and triosephosphate isomerase were enriched in the sample from cells exposed to H_2O_2. These, perhaps unexpected, smaller proteins may be present as they also form disulfide complexes in response to oxidant treatment of cardiac myocytes (30). Prdx 1 and Prdx 2 were also identified as potential DJ-1 binding partners in response to H_2O_2 treatment. However, when we performed detailed follow-up analysis of the disulfide interaction of DJ-1 with these Prdx isoforms (see below), no independent corroboration of an interaction with Prdx 1 could be found. Thus the primary focus of this study was on Prdx 2 and its oxidant-induced complexation with DJ-1. The efficiency of the IP was checked by running the soluble cell lysate, labelled input on **Fig. 3A**, together with the immunoprecipitated material on the same gel. Silver staining the gel highlighted a ~25 kDa band, corresponding with the molecular weight of the DJ-1 monomer, present in the IP samples (**Fig. 3A**). This putative enrichment of DJ-1 in the immunoprecipitate was subsequently validated by western blot (**Fig. 3B**). Prdx 2 was also detected in the DJ-1 immunoprecipitated samples from cardiomyocytes, but there was more co-capture of the Prdx when cells had been exposed to H_2O_2. Proximity Ligation Assay analysis corroborated the results obtained by western immunoblotting, showing that DJ-1 and Prdx co-localise in situ in cardiomyocytes following exposure to H_2O_2 (**Fig. 3C**).

Potentiated interprotein disulfide bond formation and Cys106 hyperoxidation in C53A DJ-1

To determine whether the redox state of a thiol in DJ-1 impacted on the susceptibility of others to oxidation, the responses of C53A or C106A DJ-1 'redox dead' mutants in response to H_2O_2 were examined. WT, C53A or C106A DJ-1 was expressed in HEK cells, which were then treated with H_2O_2. WT or C53A, but not the Cys106A mutant, formed an array of disulfide bonds with target proteins following H_2O_2 treatment (**Fig. 4A**). Surprisingly, the C53A mutant showed potentiated levels of interprotein disulfide bond formation with target proteins following H_2O_2 treatment compared to WT. This exacerbated response of the C53A DJ-1 mutant to H_2O_2 was especially apparent when it was immunoprecipitated via its V5-tag beads, resolved on a gel and silver stained. It was evident that a large number of proteins co-purified with C53A DJ-1 after cells were exposed to H_2O_2 (**Fig. 4B**).

The C53A mutant is also more susceptible to Cys106 oxidation compared to the WT, consistent with the possibility that the disulfide bond between the two DJ-1 monomers may protect Cys106 from hyperoxidation (**Fig. 4A**). Double immunofluorescence studies using antibodies to the V5-tag on transfected DJ-1 or to that which hyperoxidised (SO_3H-Cys106) further corroborated the findings based on co-immunoprecipitation. Thus, SO_3-Cys106 immunolabelling was only observed in HEK 293 cells treated with H_2O_2 if they were transfected with C53A DJ-1 mutant (**Fig. 4C**). Since the Cys106 is the most reactive cysteine, the band pattern observed with the C53A mutant may correspond with disulfide bonds between the Cys106 and target proteins.

DJ-1 Cys53 is needed for its interaction with Prdx 2

To determine which of the DJ-1 cysteines is required for the interprotein disulfide linkage with the Prdx, HEK 293 cells were transfected with plasmids for WT, C53A, or C106A together with Prdx 2 and then treated with 0 or 100 µM H_2O_2. DJ-1 protein was immunoprecipitated using V5 beads and the interaction with Prdx 2 was checked by western blot analysis to assess co-purification. Prdx 2 interacted with both WT and C106A DJ-1, but not the C53A variant, implying Cys53 is critical for disulfide bond formation between both proteins (**Fig. 5A**). Although the Prdx 2/DJ-1 WT and Prdx 2/DJ-1 C106A interactions were detected in both treated and untreated cells, it was markedly higher in those cells subjected to H_2O_2 treatment. This background level of interaction may be due to a basal oxidative stress of the HEK 293 cells subjected to transfection. PLA analysis also confirmed that C53A DJ-1 and Prdx 2 do not co-localise (**Fig 5B**). Negative controls were included as **Fig S2**.

DJ-1 C53A and C106A mutants are vulnerable to cell death due to apoptosis

We next evaluated the impact of DJ-1 redox state on the viability of cells subjected to H_2O_2 treatment. HEK 293 cells were transfected

with WT or cysteine mutant DJ-1 and subsequently treated with 200 μM H_2O_2 for 18 hours. An MTT viability assay showed cells expressing C53A or C106A DJ-1 had significantly reduced viability compared to those transfected with WT protein (Fig 6A). However, the C53A mutant was the only one that showed reduced viability compared to the WT when the cells were co-transfected with Prdx 2 and then exposed to H_2O_2 (Fig 6A). The MTT assay is not able to discriminate if the cell injury was caused by apoptosis or necrosis. Thus, to monitor the impact of DJ-1 redox state on cell apoptotic responses to H_2O_2, annexin V or cleaved caspase 3 in the transfected (i.e. V5 positive) cells were monitored using flow cytometry. No differences in the expression of cleaved caspase 3 between mutant and wildtype cells were detected (**Fig 6B, 6D**). Nevertheless, a significant increase in annexin V positive cells in the Cys53 and Cys106 transfected cells was observed (**Fig 6C and 6D**).

DISCUSSION

DJ-1 is a ubiquitous redox-responsive protein with multiple functions. The human DJ-1 (PARK7) gene is mutated in rare forms of recessively inherited Parkinsonism (4), and is therefore widely studied in the neurology field. However, in recent years alterations in DJ-1 have also been associated with multiple diseases such as amyotrophic lateral sclerosis (30), various cancers (31-33) and androgen receptor regulation (34). Surprisingly, considering DJ-1 is highly expressed in the myocardium, relatively little is known about its role there. However, the hearts of DJ-1 knock-out mice are hypertrophic and susceptible to failure (35). This implies a protective role for DJ-1 in the myocardium, but the molecular basis of this remains unclear. Here we show that DJ-1 undergoes complex and dynamic redox-state changes in cardiomyocytes and cardiac tissue during different H_2O_2 treatments. This imbalance caused by excessive oxidative stress has a central role in the development of cardiomyopathies [34, 35].

In this study we observe sulfination or sulfonation of Cys106 during high levels of peroxide, consistent with this thiol reacting with H_2O_2 to generate this hyperoxidised state. Cys106 oxidation has already been proposed as a mechanism by which DJ-1 can act as a sacrificial oxidant scavenger (16). This irreversibly oxidised DJ-1 is subject to degradation, resulting in decreased expression (36). Billia and colleagues reported low levels of DJ-1 protein in hearts from patients with heart failure, but their DJ-1 mRNA levels were not altered (35). Thus, based on our experiments, we suggest hyperoxidation of cardiac DJ-1 Cys106 may serve as a posttranslational modification which triggers its degradation in patients with heart failure. We did not observe DJ-1 degradation, likely because cells were only exposed to an acute 10 minutes treatment with H_2O_2 in our study.

Previous studies have shown that Cys106 is critical for multiple roles of DJ-1 and its interaction with target proteins (18,37-39). Here we demonstrate that the redox state of Cys53 is also important in controlling Cys106 inter disulfide complex formation with target proteins. We observe a H_2O_2 dose-dependent increase of a 50 kDa complex which may correspond to DJ-1 homodimer generated by disulfide bond formation between the Cys53 from each monomer in cardiomyocytes or perfused hearts. Cys53 is 3.3 Å from the equivalent residue on the adjacent subunit (1). Although relatively close, this is still too distant for a disulfide to bridge. However, we should also consider that the structure will have some flexibility and that the distance may change with interventions that modulate the oxidation of other cysteines in DJ-1 or upon binding of partner proteins.

It is also notable that the oxidant interventions only induce a relatively small proportion of the total pool of DJ-1 to the disulfide state. However it is important to consider that such disulfides are readily reversible, and can be continuously recycled back to the reduced state. Therefore the western blots may represent a snapshot of its redox cycle, not providing any information about the turnover rate of this process. Furthermore, DJ-1 interacts with many partners, potentially generating a variety of sub-complexes that may not all respond to oxidant in the same way, potentially delimiting the stoichiometry of disulfide formation.

A limitation of this study is an inability to differentiate between sulfinic and sulfonic hyperoxidation states of Cys106 with the antibody used. Regardless of this, it is evident that a C53A DJ-1 mutant undergoes potentiated Cys106 hyperoxidation. Intriguingly H_2O_2 treatment of cells expressing C53A DJ-1 also promoted formation of hetero-interprotein disulfides with unidentified target proteins.

During oxidative stress, the isoelectric point of DJ-1 changes from 6.2 to 5.8 (40), potentially explained by formation of the acidic hyperoxidation state well established to occur at Cys106. However, a C53A DJ-1 was resistant to this oxidation-induced 'acid shift' (19), which could be explained by Cys53 hyperoxidation.

These observations are consistent with the interprotein disulfide between Cys53 on DJ-1 subunits, which are found at the dimer interface (41), negatively regulating the susceptibility of Cys106 to hyperoxidation. This Cys53-Cys53 homo-disulfide dimer also serves to limit disulfide interactions of DJ-1 with other proteins. This leads to the rational suggestion that in the absence of a Cys53-Cys53 homo-disulfide, Cys106 has enhanced susceptibility to oxidation or disulfide formation with other proteins, perhaps because it becomes more accessible for such interactions. Such a rationale would explain why ASK1 (apoptosis signal-regulating kinase) was constitutively bound to C53A DJ-1 via Cys106 (39). Structural changes induced by DJ-1 disulfide dimer formation may impact on the redox activity of Cys106, and its capacity to form hetero- disulfide protein complexes. DJ-1 Cys106 forms disulfide bonds with multiple target proteins to limit oxidant-induced cell death (4,14,16,42), thus when this residue hyperoxidises it may lose its capacity to participate in this protective pathway. Our results showed that both Cys106 and Cys53 are important in the protective role of DJ-1 against apoptosis. Thus, the C106A mutant may promote injury because it cannot directly interact with proteins that otherwise may limit cell death, whilst the C53A mutant indirectly produces the same effect by promoting Cys106 hyperoxidation.

One of the principal observations in this study was the formation of a 75 kDa DJ-1 complex prior to the appearance of the disulfide dimeric homodimer. Mass spectrometry analysis suggested this DJ-1 complex contained Prdx2, which was subsequently corroborated by co-immunoprecipitation studies, as well as PLA analysis showing that DJ-1 Cys53 was crucial for this interaction. Typical 2-Cys Prdx, such as Prdx 2, have a peroxidatic cysteine with a very low pKa, which in the presence of H_2O_2 is oxidized to a sulfenic acid and then attacked by a resolving cysteine located in other subunit. This reaction results in the formation of a stable intersubunit disulfide bond which is reduced by thioredoxin and constitutes a mechanism of degrading H_2O_2. The low p*K*a of the peroxidatic cysteine of peroxiredoxins does not fully explain its unusually high reactivity with peroxide. Four conserved amino acids in the active site of all peroxiredoxins help stabilize the transition state of the peroxidatic S_N2 displacement reaction to enhance catalysis (43). This high reactivity with H_2O_2, together with their high abundance, may explain the importance of Prdxs as redox sensors and transducers within cells. Andres-Mateos and colleagues described DJ-1 as an "atypical peroxiredoxin like peroxidase". They estimated that the reaction of H_2O_2 with DJ-1 was at least a thousand times slower than with typical Prdxs. Indeed, H_2O_2 reacted with DJ-1 at 0.56±0.05 $M^{-1}.s^{-1}$, whereas Prdxs reacted with the same substrate between $2x10^5$ and $1.8x10^8$ $M^{-1}.s^{-1}$ (16,44,45). Due to the vastly different kinetics of these reactions we suggest that H_2O_2 selectively oxidised Prdx which acts as intracellular messenger of the oxidant signal by generating intermediate disulfide bond complexes with redox sensitive proteins such as DJ-1. Thus, we propose a model in which the Cys53 thiol of DJ-1 attacks the Prdx disulfide dimer yielding a transitional trimeric intermediate. This trimeric intermediate is abolished under higher levels of peroxide leading to the formation of DJ-1 disulfide dimer between the Cys53 residues of both DJ-1 (**Fig. 7**). This model also explains the 75 kDa complex abrogation under high levels of peroxide, which is likely due to Prdx 2 hyperoxidation.

Nuclear factor (erythroid-derived 2)-like 2 (Nrf2) activation has been associated with Prdx2 (46) and DJ-1 (47) in two independent studies. It is interesting to speculate that the disulfide interaction of Prdx2 and DJ-1 observed in this study could impact on Nrf2-dependent signalling, for example perhaps by modulating oxidation of the regulatory thiols in kelch-like ECH-associated protein (keap) 1. The interaction of DJ-1 with Prdx 1 and 6 has also been previously observed (48), although this was not increased by H_2O_2 treatment. A non-covalent association of DJ-1 and 6 would perhaps logically explain why it is able to form the hetero-disulfide dimer, which is unlikely unless DJ-1 Cys53 is very abundant and highly reactive. A non-covalent interaction of Prdx and DJ-1 may result from them being similar sized proteins that each from higher order oligomers. Indeed both Prdx and DJ-1 show overlap in function, each

having both peroxidase (16,25) and molecular chaperone activities (9,22). The Cys53 DJ-1 mediated interaction with Prdx2 is especially notable as most of the studies focus on Cys106-mediated disulfide interactions with target proteins. However Cys53 of DJ-1 is also known to be redox regulated, with its reduction being mediated by Trx (49), which is consistent with our observation that Trx reductase inhibition by auranofin induces the disulfide dimer.

Oxidant-induced apoptosis has been widely observed to occur as either a cause or a consequence of distinct pathologies including cancer, autoimmune disease, neurodegeneration and heart disease. This induction of apoptosis by oxidants is likely to be mediated, at least in part, by alterations to redox active proteins whose activity are modulated by such oxidative post-translational modifications. Prdxs are already known to induce disulfide bond formation in other proteins thereby modulating their activities, for example protein disulfide isomerase (50), or STAT3 transcription factor (28). Here, we show that DJ-1 is also such a protein, undergoing complex, multi-faceted and dynamic redox-dependent alterations that are critical for induction of oxidant-induced apoptosis. The role of DJ-1 in cell death and apoptosis has been widely studied, with it complexing with several regulators of cell survival. Indeed, some of these proteins, such as ASK1(14), Nrf2(51), PTEN (52) and Akt (53), are also thiol redox-state regulated. Our data indicate that formation of DJ-1 Cys106 disulfide linkage complexes is regulated by Cys53 oxidation and both cysteines are critical for the protective role of DJ-1. Additionally, we observed an oxidant-induced interaction between DJ-1 and Prdx 2. This transient interaction between the two proteins may reflect an oxidant sensing and transduction event, allowing post-translational regulation of DJ-1 function that is important in cellular responses to oxidative stress. Improving our understanding of the complexities of the redox regulation of DJ-1 is warranted as they may be important in the maintenance of health or the development of several diseases.

ACKNOWLEDGEMENTS

This work was supported by the European Research Council (ERC Advanced award), British Heart Foundation, Medical Research Council and Fondation Leducq, and the Department of Health via the NIHR cBRC award to Guy's & St Thomas' NHS Foundation Trust. There are no conflicts of interest to disclosure.

CONFLICT OF INTEREST

We have no conflict of interest to declare.

AUTHOR CONTRIBUTIONS

PE conceived and coordinated the study and wrote the paper. MFC wrote the paper and designed, performed and analyzed the experiments shown in Figures 1,2,3,4,5 and 6. ES designed and developed the SO3H-Cys106 DJ-1antibody and wrote the manuscript. HC designed and performed the flow cytometry experiments shown in Figure 6. JB provided technical assistance with the expression of mutant proteins. JBB and MM provided technical assistance with the mass spectrometry analysis. All authors reviewed the final version of the manuscript.

REFERENCES

1. Tao, X., and Tong, L. (2003) Crystal structure of human DJ-1, a protein associated with early onset Parkinson's disease. *The Journal of biological chemistry* **278**, 31372-31379
2. Nagakubo, D., Taira, T., Kitaura, H., Ikeda, M., Tamai, K., Iguchi-Ariga, S. M., and Ariga, H. (1997) DJ-1, a novel oncogene which transforms mouse NIH3T3 cells in cooperation with ras. *Biochemical and biophysical research communications* **231**, 509-513
3. Bonifati, V., Rizzu, P., Squitieri, F., Krieger, E., Vanacore, N., van Swieten, J. C., Brice, A., van Duijn, C. M., Oostra, B., Meco, G., and Heutink, P. (2003) DJ-1(PARK7), a novel gene for autosomal recessive, early onset parkinsonism. *Neurol Sci* **24**, 159-160
4. Bonifati, V., Rizzu, P., van Baren, M. J., Schaap, O., Breedveld, G. J., Krieger, E., Dekker, M. C., Squitieri, F., Ibanez, P., Joosse, M., van Dongen, J. W., Vanacore, N., van Swieten, J. C., Brice, A., Meco, G., van Duijn, C. M., Oostra, B. A., and Heutink, P. (2003) Mutations in the DJ-1 gene associated with autosomal recessive early-onset parkinsonism. *Science* **299**, 256-259
5. Basak, I., Pal, R., Patil, K. S., Dunne, A., Ho, H. P., Lee, S., Peiris, D., Maple-Grodem, J., Odell, M., Chang, E. J., Larsen, J. P., and Moller, S. G. (2014) Arabidopsis AtPARK13, which confers thermotolerance, targets misfolded proteins. *The Journal of biological chemistry* **289**, 14458-14469
6. Mitsugi, H., Niki, T., Takahashi-Niki, K., Tanimura, K., Yoshizawa-Kumagaye, K., Tsunemi, M., Iguchi-Ariga, S. M., and Ariga, H. (2013) Identification of the recognition sequence and target proteins for DJ-1 protease. *FEBS letters* **587**, 2493-2499
7. Chen, J., Li, L., and Chin, L. S. (2010) Parkinson disease protein DJ-1 converts from a zymogen to a protease by carboxyl-terminal cleavage. *Hum Mol Genet* **19**, 2395-2408
8. Culleton, B. A., Lall, P., Kinsella, G. K., Doyle, S., McCaffrey, J., Fitzpatrick, D. A., and Burnell, A. M. (2015) A role for the Parkinson's disease protein DJ-1 as a chaperone and antioxidant in the anhydrobiotic nematode Panagrolaimus superbus. *Cell Stress Chaperones* **20**, 121-137
9. Girotto, S., Cendron, L., Bisaglia, M., Tessari, I., Mammi, S., Zanotti, G., and Bubacco, L. (2014) DJ-1 is a copper chaperone acting on SOD1 activation. *The Journal of biological chemistry* **289**, 10887-10899

10. Cao, J., Ying, M., Xie, N., Lin, G., Dong, R., Zhang, J., Yan, H., Yang, X., He, Q., and Yang, B. (2014) The oxidation states of DJ-1 dictate the cell fate in response to oxidative stress triggered by 4-hpr: autophagy or apoptosis? *Antioxidants & redox signaling* **21**, 1443-1459
11. Pantcheva, P., Elias, M., Duncan, K., Borlongan, C. V., Tajiri, N., and Kaneko, Y. (2014) The role of DJ-1 in the oxidative stress cell death cascade after stroke. *Neural Regen Res* **9**, 1430-1433
12. Milani, P., Ambrosi, G., Gammoh, O., Blandini, F., and Cereda, C. (2013) SOD1 and DJ-1 converge at Nrf2 pathway: a clue for antioxidant therapeutic potential in neurodegeneration. *Oxidative medicine and cellular longevity* **2013**, 836760
13. Joselin, A. P., Hewitt, S. J., Callaghan, S. M., Kim, R. H., Chung, Y. H., Mak, T. W., Shen, J., Slack, R. S., and Park, D. S. (2012) ROS-dependent regulation of Parkin and DJ-1 localization during oxidative stress in neurons. *Hum Mol Genet* **21**, 4888-4903
14. Im, J. Y., Lee, K. W., Junn, E., and Mouradian, M. M. (2010) DJ-1 protects against oxidative damage by regulating the thioredoxin/ASK1 complex. *Neurosci Res* **67**, 203-208
15. Martinat, C., Shendelman, S., Jonason, A., Leete, T., Beal, M. F., Yang, L., Floss, T., and Abeliovich, A. (2004) Sensitivity to oxidative stress in DJ-1-deficient dopamine neurons: an ES- derived cell model of primary Parkinsonism. *PLoS biology* **2**, e327
16. Andres-Mateos, E., Perier, C., Zhang, L., Blanchard-Fillion, B., Greco, T. M., Thomas, B., Ko, H. S., Sasaki, M., Ischiropoulos, H., Przedborski, S., Dawson, T. M., and Dawson, V. L. (2007) DJ-1 gene deletion reveals that DJ-1 is an atypical peroxiredoxin-like peroxidase. *Proceedings of the National Academy of Sciences of the United States of America* **104**, 14807-14812
17. van der Brug, M. P., Blackinton, J., Chandran, J., Hao, L. Y., Lal, A., Mazan-Mamczarz, K., Martindale, J., Xie, C., Ahmad, R., Thomas, K. J., Beilina, A., Gibbs, J. R., Ding, J., Myers, A. J., Zhan, M., Cai, H., Bonini, N. M., Gorospe, M., and Cookson, M. R. (2008) RNA binding activity of the recessive parkinsonism protein DJ-1 supports involvement in multiple cellular pathways. *Proceedings of the National Academy of Sciences of the United States of America* **105**, 10244-10249
18. Canet-Aviles, R. M., Wilson, M. A., Miller, D. W., Ahmad, R., McLendon, C., Bandyopadhyay, S., Baptista, M. J., Ringe, D., Petsko, G. A., and Cookson, M. R. (2004) The Parkinson's disease protein DJ-1 is neuroprotective due to cysteine-sulfinic acid-driven mitochondrial localization. *Proceedings of the National Academy of Sciences of the United States of America* **101**, 9103-9108
19. Taira, T., Saito, Y., Niki, T., Iguchi-Ariga, S. M., Takahashi, K., and Ariga, H. (2004) DJ-1 has a role in antioxidative stress to prevent cell death. *EMBO reports* **5**, 213-218
20. Bandyopadhyay, S., and Cookson, M. R. (2004) Evolutionary and functional relationships within the DJ1 superfamily. *BMC Evol Biol* **4**, 6
21. Witt, A. C., Lakshminarasimhan, M., Remington, B. C., Hasim, S., Pozharski, E., and Wilson, M. A. (2008) Cysteine pKa depression by a protonated glutamic acid in human DJ-1. *Biochemistry* **47**, 7430-7440
22. Shendelman, S., Jonason, A., Martinat, C., Leete, T., and Abeliovich, A. (2004) DJ-1 is a redox-dependent molecular chaperone that inhibits alpha-synuclein aggregate formation. *PLoS biology* **2**, e362
23. Rehder, D. S., and Borges, C. R. (2010) Cysteine sulfenic acid as an intermediate in disulfide bond formation and nonenzymatic protein folding. *Biochemistry* **49**, 7748-7755
24. Wood, Z. A., Schroder, E., Robin Harris, J., and Poole, L. B. (2003) Structure, mechanism and regulation of peroxiredoxins. *Trends in biochemical sciences* **28**, 32-40
25. Perkins, A., Nelson, K. J., Parsonage, D., Poole, L. B., and Karplus, P. A. (2015) Peroxiredoxins: guardians against oxidative stress and modulators of peroxide signaling. *Trends in biochemical sciences* **40**, 435-445
26. Poynton, R. A., and Hampton, M. B. (2014) Peroxiredoxins as biomarkers of oxidative stress. *Biochimica et biophysica acta* **1840**, 906-912

27. Zito, E., Melo, E. P., Yang, Y., Wahlander, A., Neubert, T. A., and Ron, D. (2010) Oxidative protein folding by an endoplasmic reticulum-localized peroxiredoxin. *Molecular cell* **40**, 787-797
28. Sobotta, M. C., Liou, W., Stocker, S., Talwar, D., Oehler, M., Ruppert, T., Scharf, A. N., and Dick, T. P. (2015) Peroxiredoxin-2 and STAT3 form a redox relay for H2O2 signaling. *Nature chemical biology* **11**, 64-70
29. Gautier, C. A., Corti, O., and Brice, A. (2014) Mitochondrial dysfunctions in Parkinson's disease. *Rev Neurol (Paris)* **170**, 339-343
30. Lev, N., Ickowicz, D., Barhum, Y., Melamed, E., and Offen, D. (2009) DJ-1 changes in G93A-SOD1 transgenic mice: implications for oxidative stress in ALS. *Journal of molecular neuroscience : MN* **38**, 94-102
31. Lee, H., Choi, S. K., and Ro, J. Y. (2012) Overexpression of DJ-1 and HSP90alpha, and loss of PTEN associated with invasive urothelial carcinoma of urinary bladder: Possible prognostic markers. *Oncology letters* **3**, 507-512
32. Hod, Y. (2004) Differential control of apoptosis by DJ-1 in prostate benign and cancer cells. *Journal of cellular biochemistry* **92**, 1221-1233
33. Miyajima, Y., Sato, Y., Oka, H., Utsuki, S., Kondo, K., Tanizaki, Y., Nagashio, R., Tsuchiya, B., Okayasu, I., and Fujii, K. (2010) Prognostic significance of nuclear DJ-1 expression in astrocytoma. *Anticancer Res* **30**, 265-269
34. Niki, T., Takahashi-Niki, K., Taira, T., Iguchi-Ariga, S. M., and Ariga, H. (2003) DJBP: a novel DJ-1-binding protein, negatively regulates the androgen receptor by recruiting histone deacetylase complex, and DJ-1 antagonizes this inhibition by abrogation of this complex. *Mol Cancer Res* **1**, 247-261
35. Billia, F., Hauck, L., Grothe, D., Konecny, F., Rao, V., Kim, R. H., and Mak, T. W. (2013) Parkinson-susceptibility gene DJ-1/PARK7 protects the murine heart from oxidative damage in vivo. *Proceedings of the National Academy of Sciences of the United States of America* **110**, 6085-6090
36. Duan, X., Kelsen, S. G., and Merali, S. (2008) Proteomic analysis of oxidative stress-responsive proteins in human pneumocytes: insight into the regulation of DJ-1 expression. *Journal of proteome research* **7**, 4955-4961
37. Kinumi, T., Kimata, J., Taira, T., Ariga, H., and Niki, E. (2004) Cysteine-106 of DJ-1 is the most sensitive cysteine residue to hydrogen peroxide-mediated oxidation in vivo in human umbilical vein endothelial cells. *Biochemical and biophysical research communications* **317**, 722-728
38. Meulener, M. C., Xu, K., Thomson, L., Ischiropoulos, H., and Bonini, N. M. (2006) Mutational analysis of DJ-1 in Drosophila implicates functional inactivation by oxidative damage and aging. *Proceedings of the National Academy of Sciences of the United States of America* **103**, 12517-12522
39. Waak, J., Weber, S. S., Gorner, K., Schall, C., Ichijo, H., Stehle, T., and Kahle, P. J. (2009) Oxidizable residues mediating protein stability and cytoprotective interaction of DJ-1 with apoptosis signal-regulating kinase 1. *The Journal of biological chemistry* **284**, 14245-14257
40. Mitsumoto, A., Nakagawa, Y., Takeuchi, A., Okawa, K., Iwamatsu, A., and Takanezawa, Y. (2001) Oxidized forms of peroxiredoxins and DJ-1 on two-dimensional gels increased in response to sublethal levels of paraquat. *Free radical research* **35**, 301-310
41. Honbou, K., Suzuki, N. N., Horiuchi, M., Niki, T., Taira, T., Ariga, H., and Inagaki, F. (2003) The crystal structure of DJ-1, a protein related to male fertility and Parkinson's disease. *The Journal of biological chemistry* **278**, 31380-31384
42. Aleyasin, H., Rousseaux, M. W., Phillips, M., Kim, R. H., Bland, R. J., Callaghan, S., Slack, R. S., During, M. J., Mak, T. W., and Park, D. S. (2007) The Parkinson's disease gene DJ-1 is also a key regulator of stroke-induced damage. *Proceedings of the National Academy of Sciences of the United States of America* **104**, 18748-18753

43. Hall, A., Nelson, K., Poole, L. B., and Karplus, P. A. (2011) Structure-based insights into the catalytic power and conformational dexterity of peroxiredoxins. *Antioxidants & redox signaling* **15**, 795-815
44. Dubuisson, M., Vander Stricht, D., Clippe, A., Etienne, F., Nauser, T., Kissner, R., Koppenol, W. H., Rees, J. F., and Knoops, B. (2004) Human peroxiredoxin 5 is a peroxynitrite reductase. *FEBS letters* **571**, 161-165
45. Harrison, W. H., Whisler, W. W., and Hill, B. J. (1968) Catecholamine oxidation and ionization properties indicated from the H+ release, tritium exchange, and spectral changes which occur during ferricyanide oxidation. *Biochemistry* **7**, 3089-3094
46. Matte, A., De Falco, L., Iolascon, A., Mohandas, N., An, X., Siciliano, A., Leboeuf, C., Janin, A., Bruno, M., Choi, S. Y., Kim, D. W., and De Franceschi, L. (2015) The Interplay Between Peroxiredoxin-2 and Nuclear Factor-Erythroid 2 Is Important in Limiting Oxidative Mediated Dysfunction in beta-Thalassemic Erythropoiesis. *Antioxidants & redox signaling* **23**, 1284-1297
47. Clements, C. M., McNally, R. S., Conti, B. J., Mak, T. W., and Ting, J. P. (2006) DJ-1, a cancer- and Parkinson's disease-associated protein, stabilizes the antioxidant transcriptional master regulator Nrf2. *Proceedings of the National Academy of Sciences of the United States of America* **103**, 15091-15096
48. Knobbe, C. B., Revett, T. J., Bai, Y., Chow, V., Jeon, A. H., Bohm, C., Ehsani, S., Kislinger, T., Mount, H. T., Mak, T. W., St George-Hyslop, P., and Schmitt-Ulms, G. (2011) Choice of biological source material supersedes oxidative stress in its influence on DJ-1 in vivo interactions with Hsp90. *Journal of proteome research* **10**, 4388-4404
49. Fu, C., Wu, C., Liu, T., Ago, T., Zhai, P., Sadoshima, J., and Li, H. (2009) Elucidation of thioredoxin target protein networks in mouse. *Molecular & cellular proteomics : MCP* **8**, 1674-1687
50. Tavender, T. J., Springate, J. J., and Bulleid, N. J. (2010) Recycling of peroxiredoxin IV provides a novel pathway for disulphide formation in the endoplasmic reticulum. *The EMBO journal* **29**, 4185-4197
51. Liu, C., Chen, Y., Kochevar, I. E., and Jurkunas, U. V. (2014) Decreased DJ-1 leads to impaired Nrf2-regulated antioxidant defense and increased UV-A-induced apoptosis in corneal endothelial cells. *Investigative ophthalmology & visual science* **55**, 5551-5560
52. Klawitter, J., Klawitter, J., Agardi, E., Corby, K., Leibfritz, D., Lowes, B. D., Christians, U., and Seres, T. (2013) Association of DJ-1/PTEN/AKT- and ASK1/p38-mediated cell signalling with ischaemic cardiomyopathy. *Cardiovasc Res* **97**, 66-76
53. Zhu, Z. M., Li, Z. R., Huang, Y., Yu, H. H., Huang, X. S., Yan, Y. F., Shao, J. H., and Chen, H. P. (2014) DJ-1 is involved in the peritoneal metastasis of gastric cancer through activation of the Akt signaling pathway. *Oncology reports* **31**, 1489-1497

FIGURE LEGENDS

FIGURE 1. Effect of H_2O_2 on the redox state of cardiac DJ-1. Non-reducing immunoblots of cardiomyocytes or rat heart were probed with anti-DJ-1, anti-DJ-1 Cys106SO_3H or 2 Cys PrdxSO_3 antibodies under reducing (R) or non-reducing (NR) conditions. A, Cardiomyocytes were treated with 0-200 µM H_2O_2 for 10 min. B, Rat hearts were perfused with 0-500 µM H_2O_2 or 1mM diamide. C, Cardiomyocytes were treated for 30 min with 1-3 µg auranofin followed by treatment with 100 µM H_2O_2 for 10 min.

FIGURE 2. A, Annotated MS/MS spectra for peptide GLFIIDAK of rat Prdx 2 detected after immunoprecipitation of DJ-1 from cardiomyocytes treated with 50 µM H_2O_2. The GLFIIDAK and QITVNDLPVGR peptides were detected two (x2) and three times (x3) respectively. B, Prdx 2 total spectrum count and Total Ion Current for each sample from three independent cardiomyocyte isolations under control conditions or exposure to 50 µM H_2O_2.

FIGURE 3. Oxidative stress promotes interaction of DJ-1 with Prdx 2. A, Silver-stained gel of DJ-1 immunoprecipitated from cardiomyocytes. B, Immunoblot showing Prdx 2 co-immunoprecipitation with DJ-1. Cardiomyocytes were treated with or without 100 µM H_2O_2, after which cell lysates were prepared and DJ-1 was immunoprecipitated and analysed by immunoblotting with an antibody to Prdx 2 or DJ-1. The Prdx 2 band is highlighted (*). IgG correspond to agarose IgG beads and IgG+Ab to IgG beads and DJ-1 antibody. C, Representative image from a Proximity Ligation Assay which allows possible protein-protein interactions between DJ-1 and Prdx 2 to be assessed. Cardiomyocytes were treated with 0 or 50 µM H_2O_2 for 10 min and then stained with antibodies to DJ-1 and Prdx 2. The nucleus was stained blue with b4′,6-diamidino-2-phenylindole (DAPI) . Each red dot represents the detection of protein-protein complexes between DJ-1 and Prdx 2, which are markedly increased following H_2O_2 treatment. Scale bar: 50 µm

FIGURE 4. C53A DJ-1 is more susceptible to H_2O_2-induced Cys106 hyperoxidation than WT. A, Non-reducing immunoblots of HEK 293 cells lysates transfected with a WT, C53A or C106A DJ-1 plasmid probed with antibodies to the V5 tag on the transfected DJ-1 or to hyperoxidised Cys106SO_3H DJ-1. HEK 293 cells were treated with 0, 100 or 500 µM H_2O_2 for 10 min. The formation of disulfide-dependent complexes as well as Cys106 hyperoxidation was significantly higher in the Cys53 mutant. Cells transfected with C106A DJ-1 were less susceptible to disulfide complex formation compared to those cells transfected with the WT protein. Statistical significance was calculated using two-way ANOVA with Bonferroni post hoc test; *** $P < 0.001$ B, Silver-stained gel of immunoprecipitated DJ-1 from transfected HEK 293 cells lysates. Mutant DJ-1 proteins (WT, C53A and C106A) were precipitated using V5 agarose beads from HEK 293 cells treated with 100 µM H_2O_2 for 10 min. C, Double immunofluorescence with V5-tag (green) and SO_3H-Cys106 DJ-1 (pink) antibodies in HEK 293 cells transfected with WT, C53A or C106A plasmids and treated with 0 or 500 µM H_2O_2 for 10 min. Scale bar: 10 µm

FIGURE 5. Prdx 2 interacts with DJ-1 Cys53. A, Immunoblot showing Prdx 2 co-immunoprecipitation with DJ-1. HEK 293 cells were transfected with WT, C53A or C106A together with Prdx 2 plasmids and then treated with 0 or 100 µM H_2O_2 for 10 min. Prdx 2 co-precipitated with WT or C106A but not with the C53A DJ-1. B, Representative image of Proximity Ligation Assay assessing protein-protein interactions between DJ-1 mutants (WT, C53A or C106A) and Prdx 2. HEK 293 cells were treated with 0 or 500 µM H_2O_2 for 10 min and then stained with anti-V5 tag and His-tag antibodies. The nucleus was stained with b4′,6-diamidino-2-phenylindole (DAPI) nuclear staining (blue). Each red dot represents the detection of protein-protein complexes between DJ-1 and Prdx 2. Scale bar: 100 µm

FIGURE 6. Expression of C53A or C106A DJ-1 enhances vulnerability to H_2O_2-induced apoptosis. A, MTT assay of HEK 293 transfected with WT, C53A or C106A DJ-1 plasmids alone or together with Prdx 2. These cells were then treated with 0 or 200 µM H_2O_2 for 18 hours. Statistical significance was calculated using two-way ANOVA with Bonferroni post hoc test; *$P < 0.05$; **$P < 0.01$; *** $P < 0.001$ B-C, Representative flow cytometry results of cell apoptosis in HEK 293 cells (V5 positive) transfected with different DJ-1 constructs (WT, C53A or C106A) using cleaved caspase 3 and Annexin V antibodies. D, Histograms represent the mean ± standard deviation of the

percentage of positive cells for cleaved caspase 3, annexin V and live/dead stained cells. HEK 293 cells were transfected with WT, C53A or C106A plasmids and treated with 0 or 200 μM H_2O_2 for 18 hours. Statistical significance was calculated using one-way ANOVA with Bonferroni post hoc test; *P < 0.05; **P < 0.01; *** P < 0.001

FIGURE 7. Hypothetical model to explain H_2O_2-induced interaction of DJ-1 and Prdx 2. In the presence of H_2O_2 the peroxidatic cysteine of peroxiredoxin residue is oxidized to sulfenic acid, which then reacts with a free thiol of a resolving cysteine located in the other Prdx monomer. At this point DJ-1 Cys53 attacks the peroxiredoxin disulfide dimer to yield a trimeric intermediate transition state. Thus, Prdx acts as a sensor and transducer of the oxidant signal by generating an intermediate disulfide bond complex with DJ-1. Finally, this trimeric structure is resolved to result in a homo interprotein disulfide bond between the Cys53 residues from each DJ-1 monomer.

Table 1. Proteins identified in 75 kDa gel bands after immunoprecipitation of DJ-1 from control or H_2O_2-treated rat ventricular cardiomyocytes

Identified Proteins	Accession Number	Molecular Weight (kDa)	P-value	QUANTITATIVE VALUE*(10^4)					
				50 μM H_2O_2			Controls		
Peroxiredoxin-1	Q63716	22	0.004	9.26	5.54	10.08	0	0	0
Peroxiredoxin-2	**P35704**	**22**	**0.050**	**7.04**	**4.34**	**1.62**	**0**	**0**	**0**
Triosephosphate isomerase	P48500	27	0.030	3.23	8.85	11.09	0	0	0
Glyceraldehyde-3-phosphate dehydrogenase	E9PTN6	36	0.002	16.99	10.46	17.08	0	0	0
Fructose-bisphosphate aldolase	G3V900	45	0.000	5.34	4.21	5.73	0	0	0
Myoglobin	Q9QZ76	17	0.023	9.76	10.67	3.91	0.33	0.87	0.34
E3 ubiquitin-protein ligase	Q6AXU4	19	0.000	0	0	0	2.87	2.73	2.26
Phosphoglucomutase 1	Q499Q4	61	0.046	195.54	230.89	192.33	154.50	177.57	132.26
Acyl-Coenzyme A dehydrogenase, very long chain	Q5M9H2	71	0.003	159.97	162.13	152.58	242.11	293.71	298.27
EH-domain containing 4	Q8R3Z7	61	0.015	88.36	76.68	79.70	63.60	51.27	42.29
Dihydrolipoyllysine-residue acetyltransferase component of pyruvate dehydrogenase complex	P08461	67	0.002	42.64	27.64	26.36	74.98	88.90	76.30
Carnitine O-palmitoyltransferase 2	P18886	74	0.035	58.55	52.97	65.49	79.91	84.58	111.53
Acyl-CoA synthetase family member 2	Q499N5	68	0.037	54.09	43.71	56.45	65.04	76.83	64.33
RCG37494	D3ZZN3	75	0.017	26.66	23.20	19.13	44.18	55.85	73.72
Rab GDP dissociation inhibitor alpha	P50398	51	0.004	24.93	29.89	36.33	12.24	7.10	63.03
Protein kinase, AMP-activated, alpha 2 catalytic subunit	G3V715	62	0.021	0	3.41	1.28	16.05	8.83	87.02
RCG23609, isoform CRA	G3V885	224	0.032	120.80	103.28	157.28	68.48	47.30	82.06
Phosphorylase	G3V8V3	97	0.049	4.10	2.01	4.30	0	2.03	0

*The quantitative value is a normalized value which takes into account the sum of the "Unweighted Spectrum Counts" for each sample analysed by mass spectrometry. The scaling factor for each immunoprecipitated sample is applied to each protein group and adjusts its "Unweighted Spectrum Count" to a normalized "Quantitative Value". Statistical significance was calculated using a t-test. Please refer to Supplemental

Figure 1

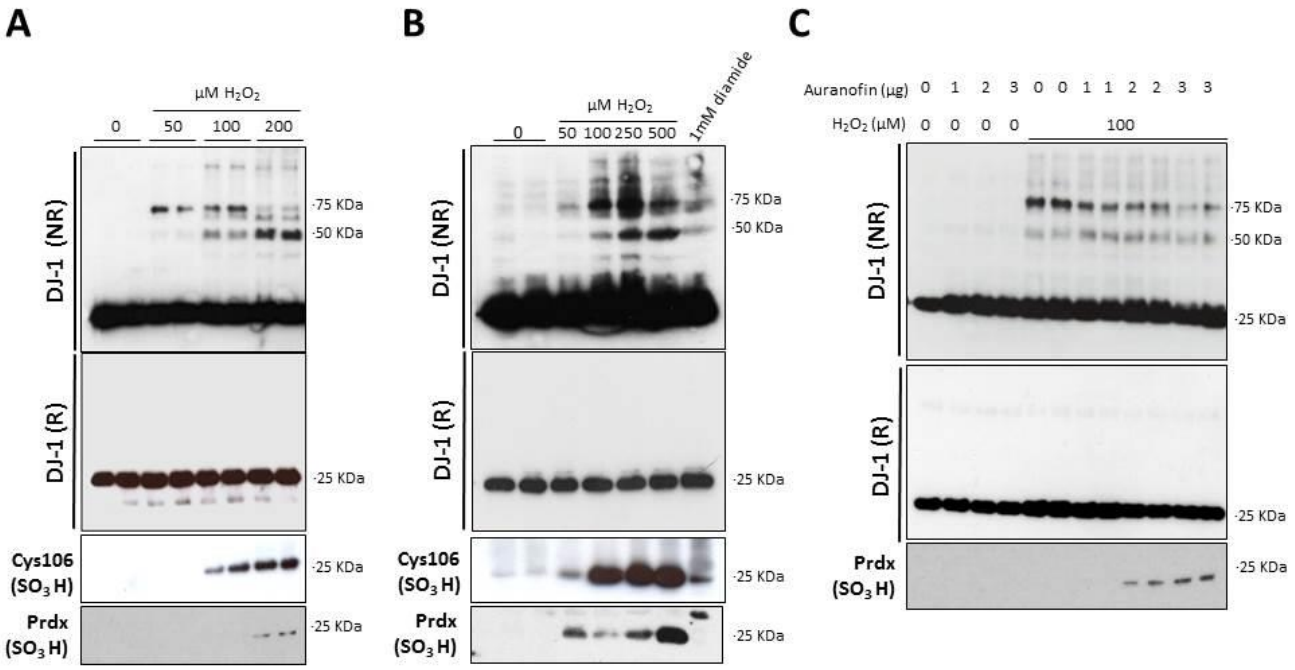

Figure 2

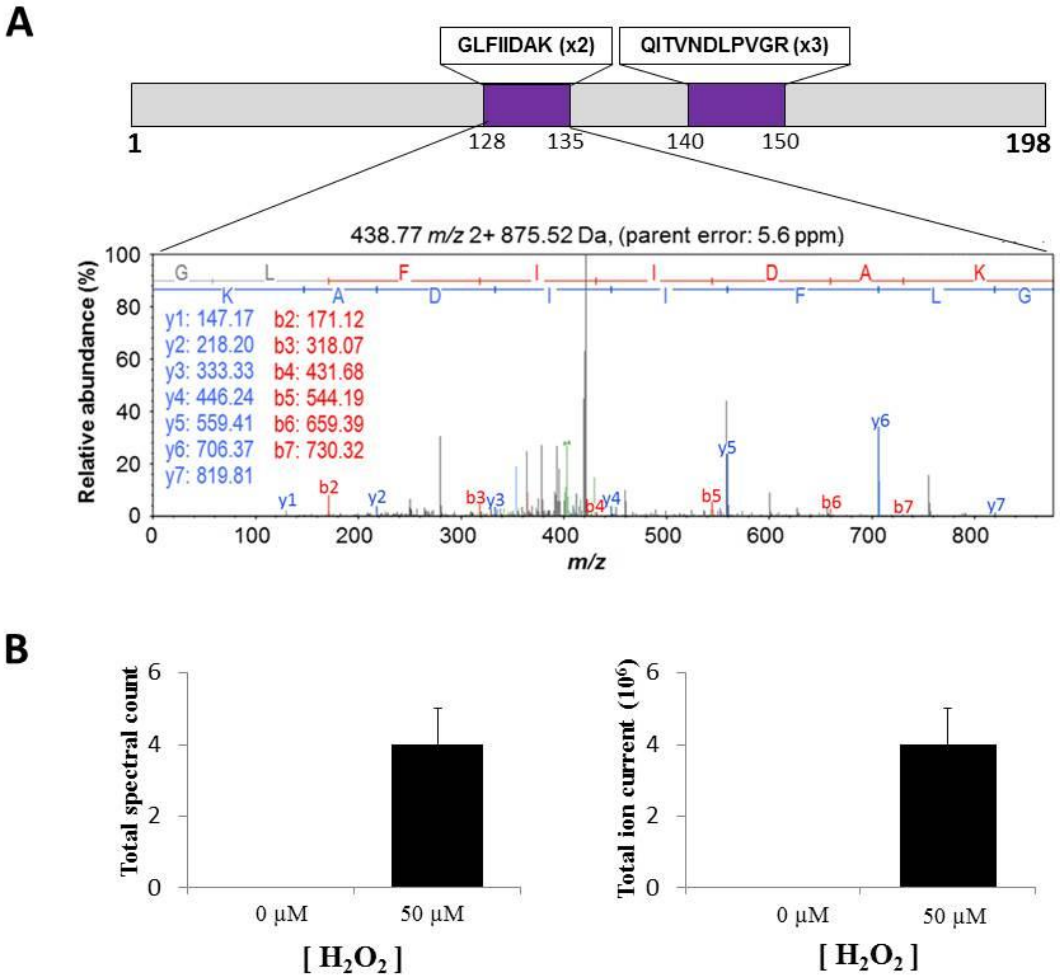

Figure 3

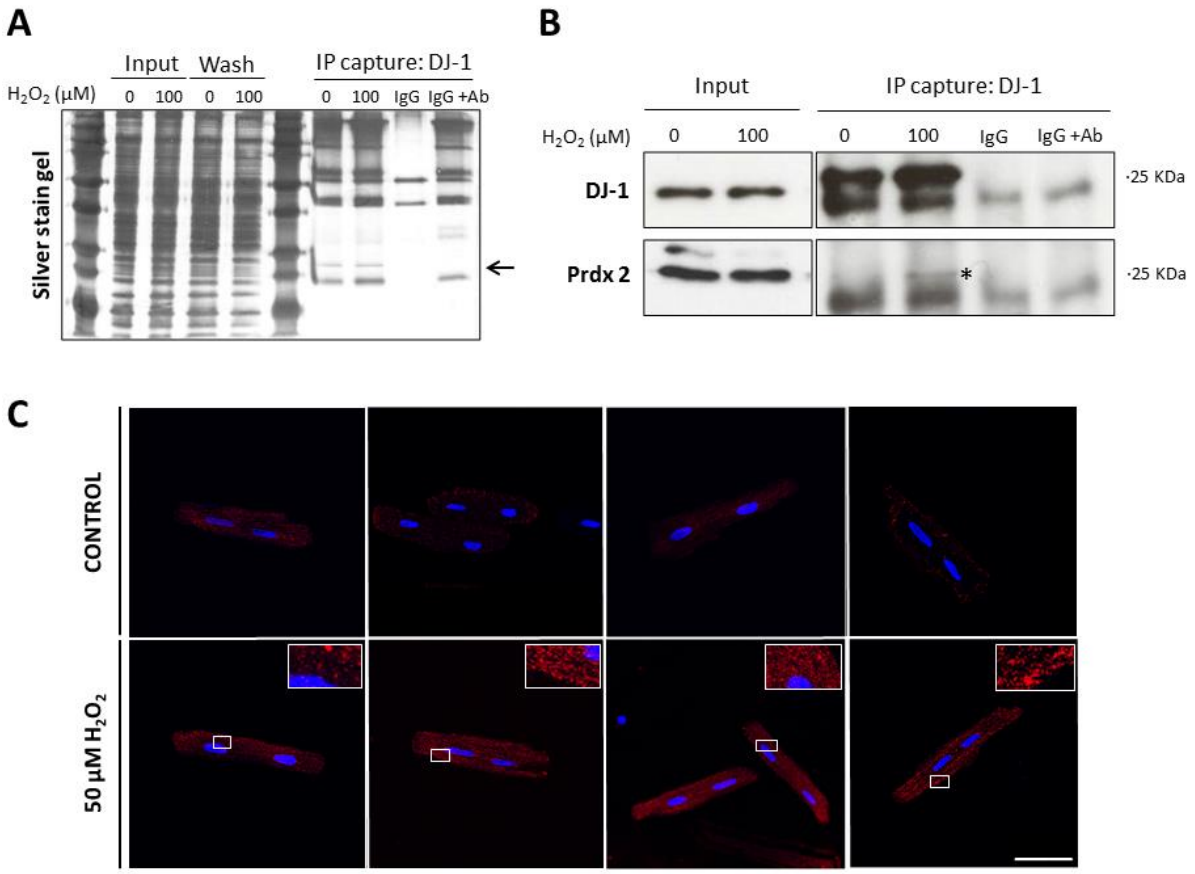

Figure 4

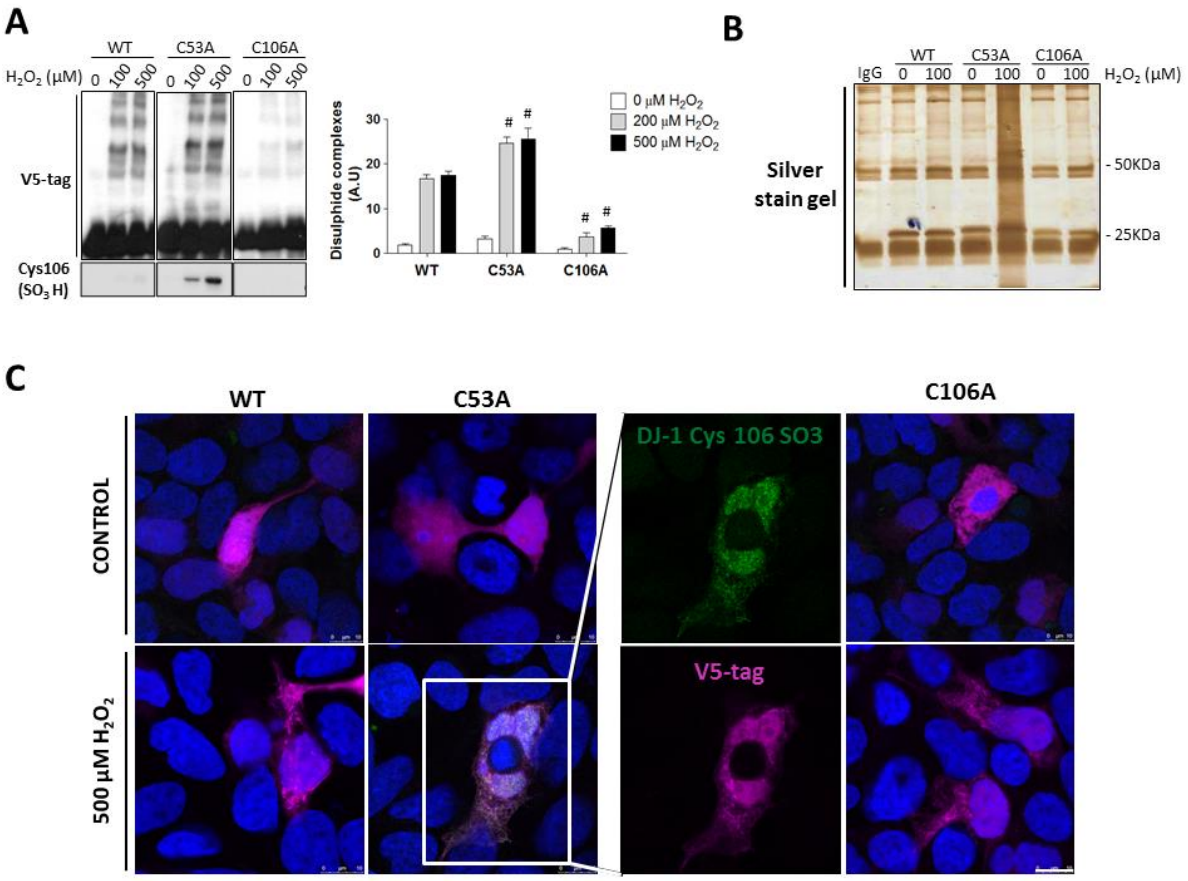

Figure 5

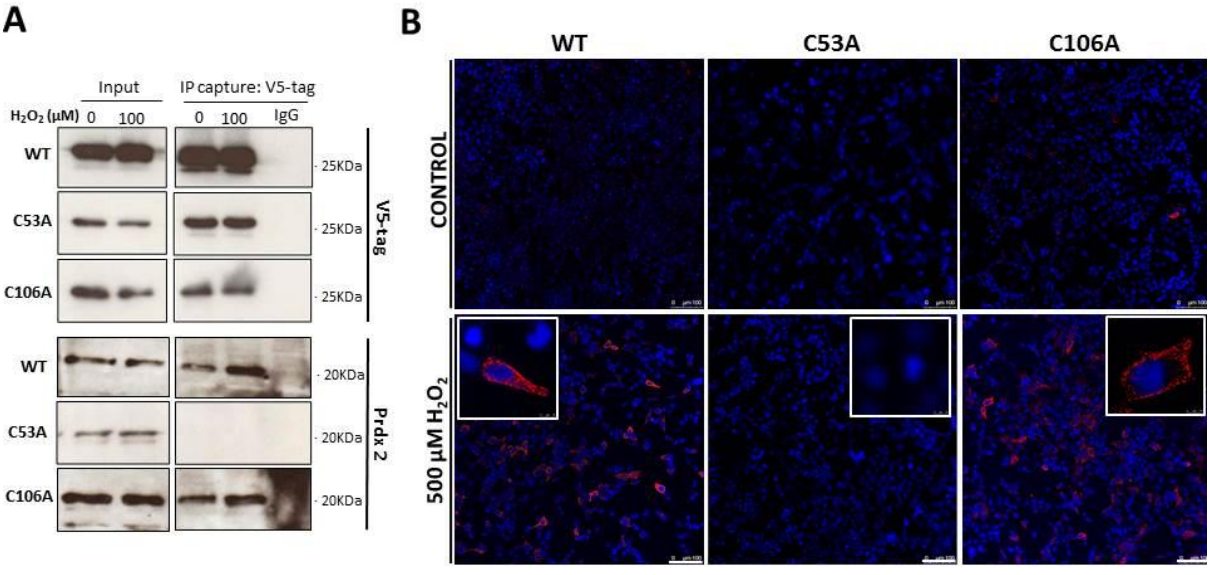

Figure 6

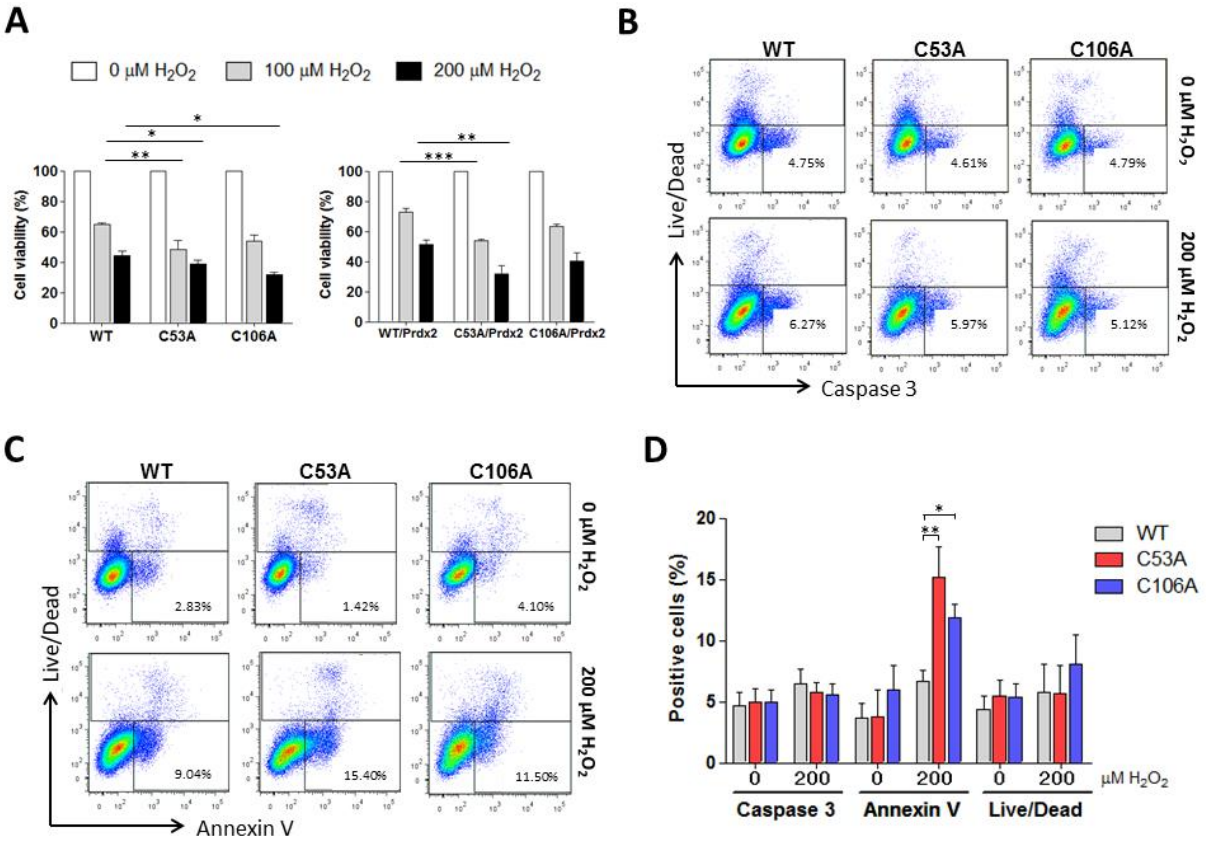

Figure 7

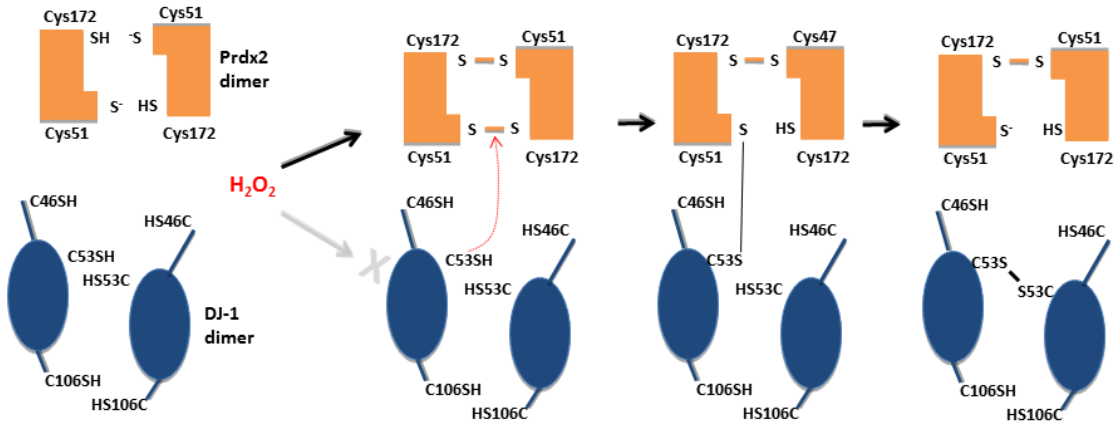

Oxidant-induced interprotein disulfide formation in cardiac DJ-1 occurs via an interaction with peroxiredoxin 2

Mariana Fernandez-Caggiano, Ewald Schroder, Hyun-Ju Cho, Joseph Burgoyne, Javier Barallobre-Barreiro, Manuel Mayr and Philip Eaton

J. Biol. Chem. published online March 4, 2016
